RSC Advances

PAPER

View Article Online
View Journal | View Issue

Cite this: *RSC Adv.*, 2024, **14**, 21763

Design, synthesis and computational studies of new azaheterocyclic coumarin derivatives as anti-*Mycobacterium tuberculosis* agents targeting enoyl acyl carrier protein reductase (InhA)†

Rasha Z. Batran, *[a] Ahmed Sabt, [a] Jarosław Dziadek[b] and Asmaa F. Kassem[c]

Received 12th April 2024
Accepted 17th June 2024

DOI: 10.1039/d4ra02746a

rsc.li/rsc-advances

In this study, we designed and synthesized a series of coumarin derivatives as antitubercular agents targeting the enoyl acyl carrier protein reductase (InhA) enzyme. Among the synthesized compounds, the tetrazole derivative **4c** showed the most potent antitubercular effect with a minimum inhibitory concentration value (MIC) of 15 μg mL^{-1} against *Mtb* H37Rv and could also inhibit the growth of the mutant strain (Δ*katG*). Compound **4c** was able to penetrate *Mtb*-infected human macrophages and suppress the intracellular growth of tubercle bacilli. Moreover, the target derivative **4c** showed a potent inhibitory effect against InhA enzyme with an IC_{50} value of 0.565 μM, which was superior to the reference InhA inhibitor triclosan. Molecular docking of compound **4c** within the InhA active site revealed the importance of the 4-phenylcoumarin ring system and tetrazole moiety for activity. Finally, the physicochemical properties and pharmacokinetic parameters of **4c** were investigated.

1. Introduction

Tuberculosis (TB), a severe respiratory infectious disease caused by *Mycobacterium tuberculosis* (*Mtb*), is considered one of the top ten global causes of mortality and is currently recognized as the world's primary cause of death from a single infectious agent, surpassing HIV/AIDS.[1–3] According to the World Health Organization (WHO), it has been estimated that about 10 million new cases of TB were diagnosed in 2021, with approximately 1.5 million deaths.[4] The increasing drug resistance of *Mycobacterium tuberculosis* strains and the limited efficacy of antitubercular therapy have contributed to the worsening epidemiological status of TB.[5,6] The emerging resistance is also exacerbated by several drawbacks of the traditional anti-TB therapies, such as long duration and use of multiple drugs, *e.g.* isoniazid (INH), ethambutol, rifampicin, fluoroquinolones and linezolid.[7,8] Resistance to rifampicin is due to mutations in the β-subunit of RNA polymerase, whereas resistance to isoniazid primarily arises from mutations in the *katG* gene[9] that encodes the catalase/peroxidase enzyme, which activates the prodrug INH inside the mycobacterial cell and enables it to bind to the active site of enoyl acyl carrier protein reductase (InhA), an essential NADH-dependent enzyme involved in mycolic acid synthesis and plays a crucial role in the survival of mycobacteria.[10] Therefore, the inhibition of *M. tuberculosis* InhA represents a significant approach for the discovery of novel anti-TB drugs that could circumvent the resistance mechanisms exerted by *Mtb* strains,[11–13] *e.g.* triclosan,[14] arylamide,[15] diphenyl ether derivatives,[16,17] 4-hydroxy-2-pyridones[18] and pyrrolidine carboxamide analogs.[19] The lack of novel remedies coming through the pipeline makes the development of new innovative strategies to cure TB an urgent challenge.

Regarding the pharmacophoric features of InhA inhibitors, three InhA key sites were observed to accommodate the inhibitors. Site I includes a tyrosine residue and the ribose group of the NAD factor. Most InhA inhibitors contain an oxygen atom that interacts with the hydroxyl group of the Tyr158 residue and the ribose ring of the NAD cofactor. Site II has a flexible hydrophobic pocket that accommodates long alkyl chains. Extending the inhibitor substrate into this pocket leads to increase in lipophilicity, which provides the benefits of ease in crossing biological membranes and hence enhanced potency. The third pocket, site III, is relatively unexplored, which offers the opportunity for hydrophilic interactions through the phosphate groups of NAD and hydrophobic interactions *via* Ala198 and Ile202 residues. The undiscovered aspect of the InhA binding pocket offers a considerable chance to modify the physicochemical properties of InhA binding scaffolds.[20–22]

[a]*Chemistry of Natural Compounds Department, Pharmaceutical and Drug Industries Research Institute, National Research Centre, Dokki, Cairo, 12622, Egypt. E-mail: rasha_batran@yahoo.com*

[b]*Laboratory of Genetics and Physiology of Mycobacterium, Institute of Medical Biology of the Polish Academy of Sciences, Lodz, Poland*

[c]*Chemistry of Natural and Microbial Products Department, Pharmaceutical and Drug Industries Research Institute, National Research Centre, Dokki, Cairo, 12622, Egypt*

† Electronic supplementary information (ESI) available. See DOI: https://doi.org/10.1039/d4ra02746a

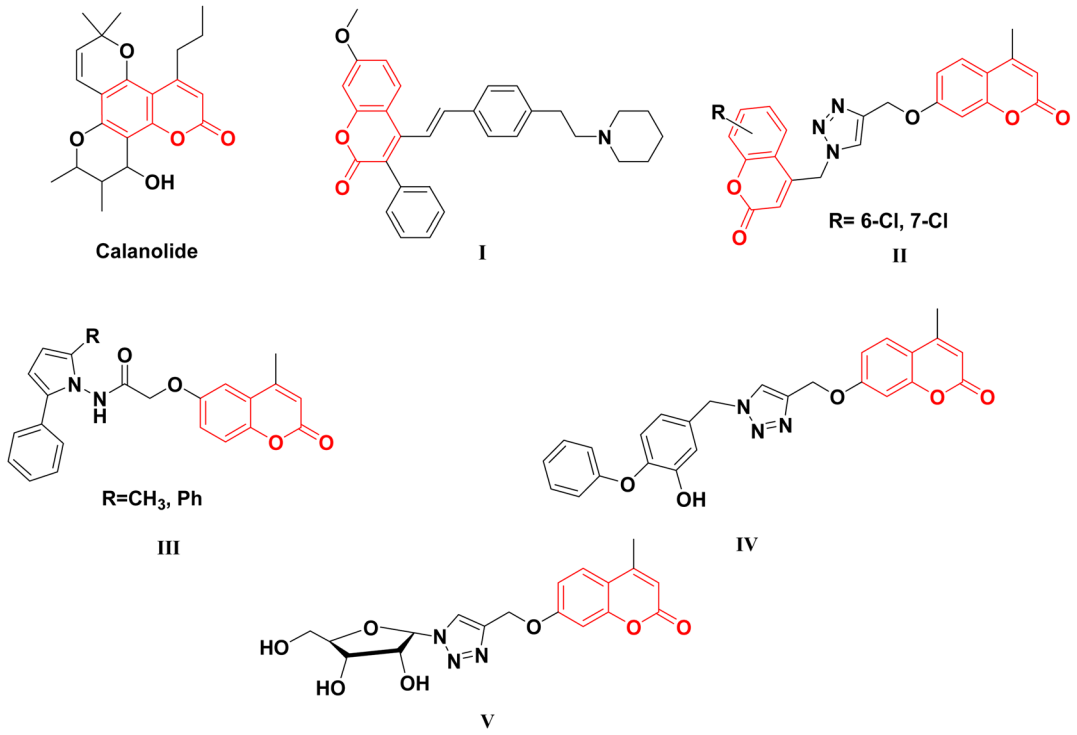

Fig. 1 Coumarin-based derivatives as anti-TB agents and InhA inhibitors.

Coumarin scaffold is a widely recognized naturally derived chemical backbone in the field of medicinal chemistry, exhibiting a diverse array of biological effects, such as anticancer,[23,24] anti-inflammatory,[25,26] antioxidant,[27,28] antimicrobial,[29,30] and, particularly, antitubercular, such as InhA inhibitory agents.[31–35] In recent years, several coumarin scaffolds have been reported for their potent anti-TB activities (Fig. 1). However, the safety profile of these compounds remains an important issue for the determination of their biological impact; for example, the naturally occurring Calanolide A displayed an anti-TB effect with an MIC value of 3.13 μg mL^{-1} and relatively low selectivity index (SI = 2.43).[34] Similarly, 3-phenyl-4-syrylcoumarin I exhibited potent anti-*Mtb* effectiveness (MIC = 3.5 μg mL^{-1}) with SI value of 2.85.[35]

The nature of the coumarin structure facilitates its engagement in various forms of interactions, including hydrogen bonding, hydrophobic interactions, and π–π stacking.[36–38] Moreover, the isosteric features of the coumarin scaffold are shared with the bioactive quinoline core, which forms the main skeleton of several FDA-approved antitubercular drugs, such as bedaquiline and fluoroquinolones, making the coumarin core an attractive target for the design and synthesis of anti-TB candidates.

Moreover, nitrogen-containing heterocycles have been recognized as privileged structures owing to their versatile

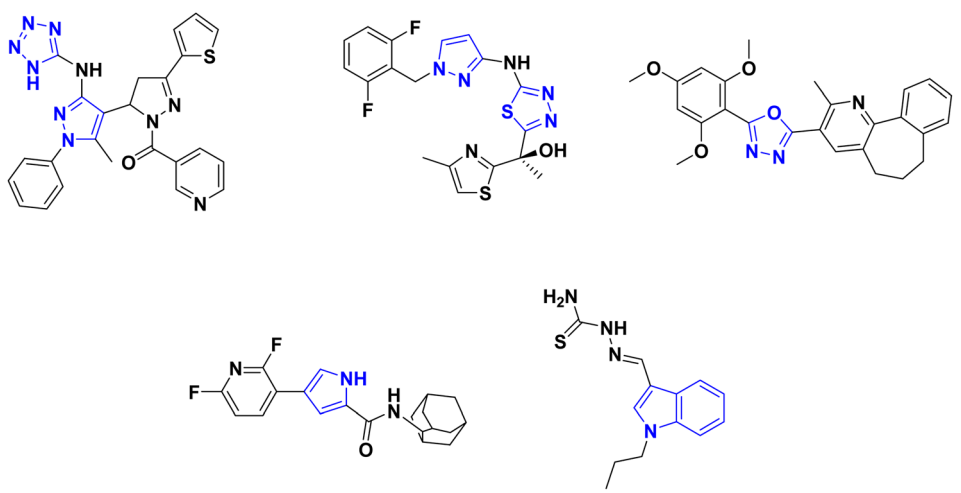

Fig. 2 Azaheterocyclic compounds showing antimycobacterial and InhA inhibition effects.

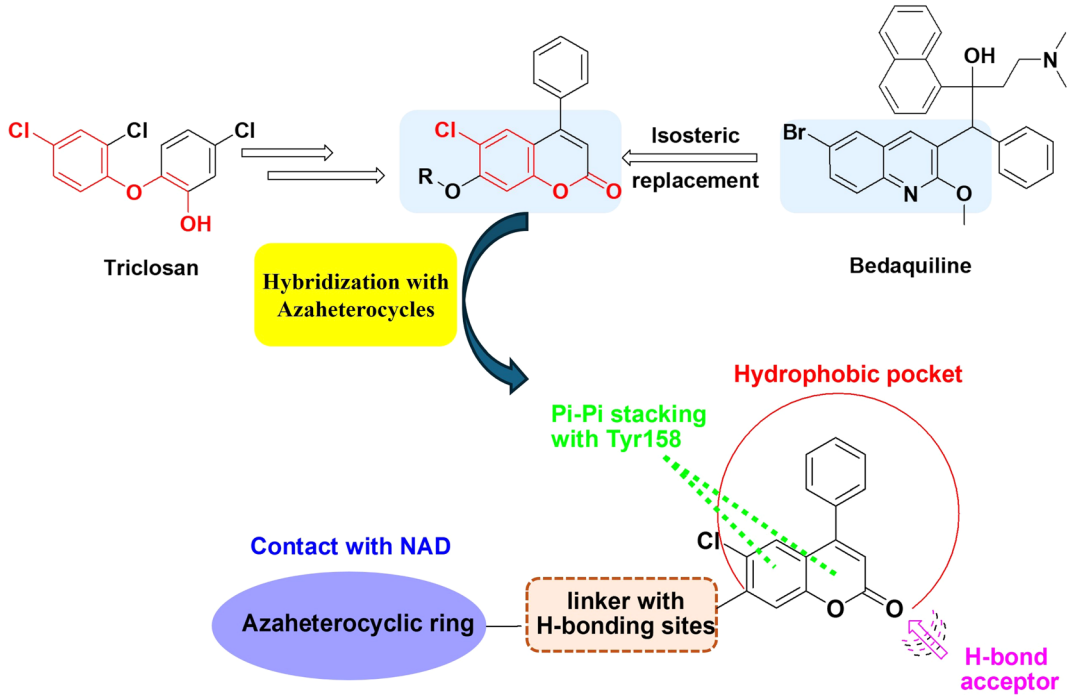

Fig. 3 Design strategy for the synthesis of coumarin-azaheterocycle hybrids and possible interaction with InhA active site.

interactions with diverse biological targets.[39,40] The five-membered azaheterocyclic molecular scaffolds, such as tetrazoles,[41] thiadiazole,[42–44] oxadiazole,[45] pyrazole[41,44,46,47] and pyrrole[48] as well as the fused nitrogen-containing heterocycles as indoles,[49,50] are encompassed in a vast number of antimycobacterial candidates endowed with InhA inhibitory effects (Fig. 2).

A molecular hybridization strategy was used in drug design and development based on the combination of different pharmacophoric moieties to afford a new hybrid entity with possibly improved affinity and efficacy and reduced undesirable side effects. In this investigation, we aimed to study the potential antitubercular effects of new azaheterocyclic coumarin hybrids against the wild type *Mtb* H37Rv and the mutant strain (Δ*katG*), targeting InhA and taking their safety profile into concern. The design of the target derivatives was rationally established by replacing the quinoline core of the FDA-approved antimycobacterial drugs, *e.g.* bedaquiline, with the coumarin isostere conserving the common pharmacophoric features of triclosan InhA inhibitor (Fig. 3). Moreover, molecular docking studies were performed to evaluate the modes of interactions between the potent derivatives and the target enzyme. The pharmacokinetic parameters of the most active compound were also studied.

2. Results and discussion

2.1. Chemistry

The synthesis of the target compounds **3**, **4a–c**, **8a–c**, **9a–c** and **10–17** was outlined in Schemes 1–4. Condensation of the starting compound 6-chloro-7-hydroxy-4-phenylcoumarin with 2-chloroacetonitrile in dry acetonitrile in the presence of anhydrous potassium carbonate afforded the corresponding 7-oxyacetonitrile derivative **2**. The heterocyclization of compound **2** to the corresponding tetrazole derivative **3** proceeded *via* a reaction with sodium azide and ammonium chloride in DMF. The reaction of tetrazole derivative **3** with 2-(dimethylamino) ethyl chloride hydrochloride, 2-(diethylamino)ethyl chloride hydrochloride, and/or 4-(2-chloroethyl) morpholine hydrochloride in dry acetonitrile in the presence of anhydrous potassium carbonate yielded the corresponding dimethylaminoethyl, diethylaminoethyl and morpholinoethyl tetrazole derivatives **4a–c**, respectively (Scheme 1).

Cyclization of the key thiosemicarbazides **7a–c** in conc. sulfuric acid at 0 °C and refluxing pyridine afforded the corresponding alkyl or phenylamino-1,3,4-thiadiazoles **8a–c** and 1,3,4-oxadiazole derivatives **9a–c**, respectively (Scheme 2).

Cyclocondensation of the hydrazide intermediate **6** with different β-dicarbonyl compounds, namely, acetylacetone, ethylacetoacetate and diethylmalonate, yielded the corresponding 3,5-dimethylpyrazole **10**, 3-methylpyrazol-5-one **11** and pyrazolidine-3,5-dione **12**, respectively. The target imides, 2,5-dioxo-2*H*-pyrrole **13** and 1,3-dioxoisoindoline **14**, were obtained by the heterocyclization of hydrazide **6** with different acid anhydrides as maleic and/or phthalic anhydride in acetic acid, respectively (Scheme 3).

Refluxing the intermediate hydrazide **6** with different indole compounds, namely, 3-indole carbaldehyde, 3-acetyl indole and/or isatin, in ethyl alcohol using a catalytic amount of glacial acetic acid afforded the corresponding Schiff's bases **15–17** (Scheme 4). The structures of the newly synthesized target

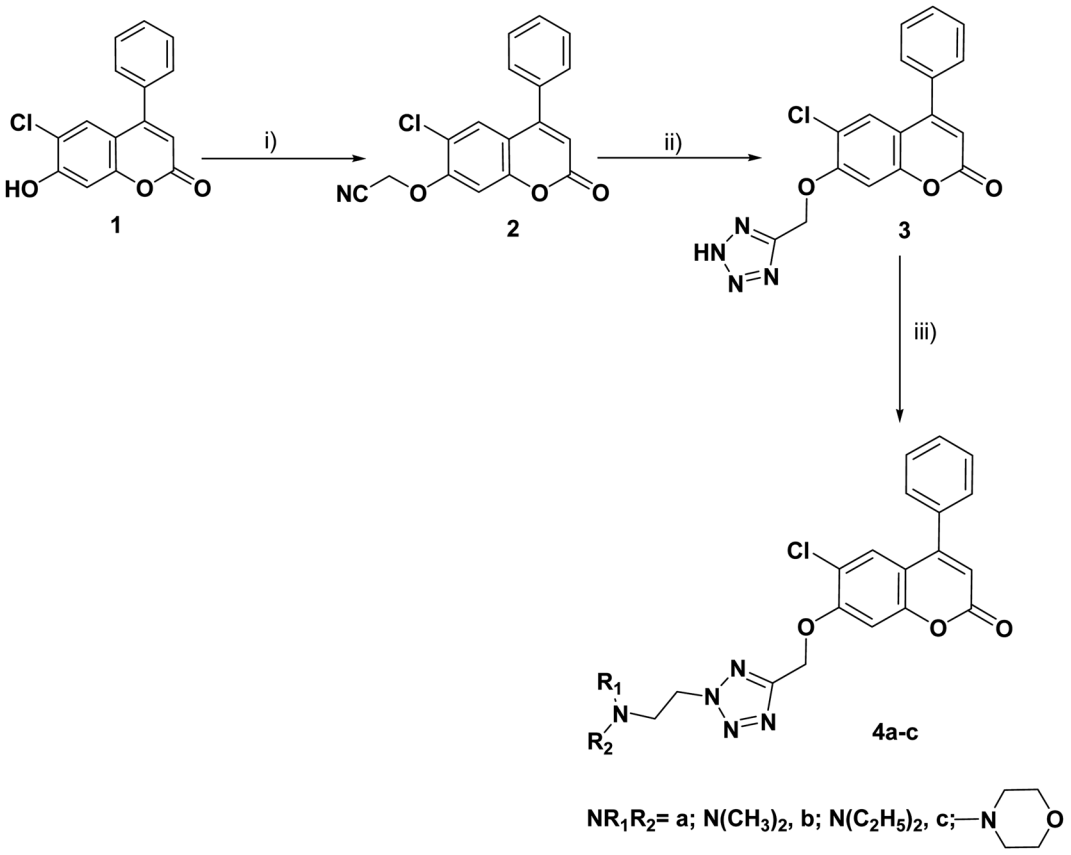

Scheme 1 Reagents and conditions: (i) $ClCH_2CN$, K_2CO_3, CH_3CN, reflux, 8 h; (ii) NH_4Cl, NaN_3, DMF, 120 °C; 7 h (iii) $ClCH_2CH_2NR_1R_2 \cdot HCl$, K_2CO_3, CH_3CN, reflux, 8–10 h.

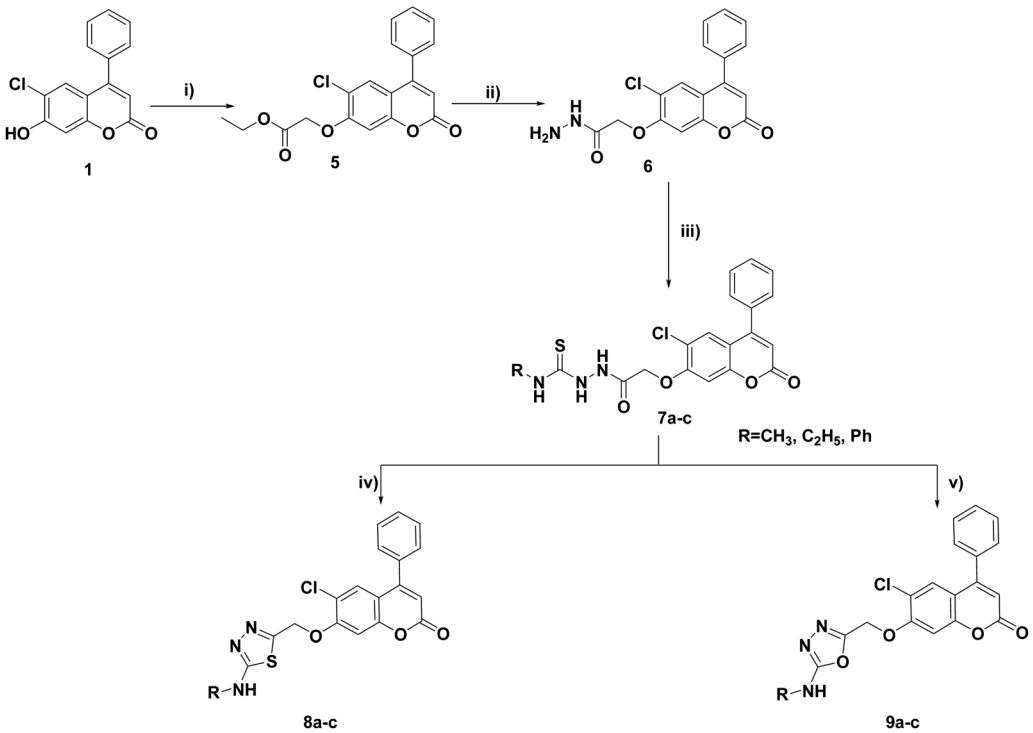

Scheme 2 Reagents and conditions: (i) $C_2H_5OCOCH_2Br$, anhydrous K_2CO_3, acetone, reflux, 8–10 h (ii) $NH_2NH_2 \cdot H_2O$, EtOH, RT, 24 h; (iii) RNCS, EtOH, reflux, 5–7 h; (iv) H_2SO_4, 0 °C, 30 min; (v) pyridine, reflux, 10–14 h.

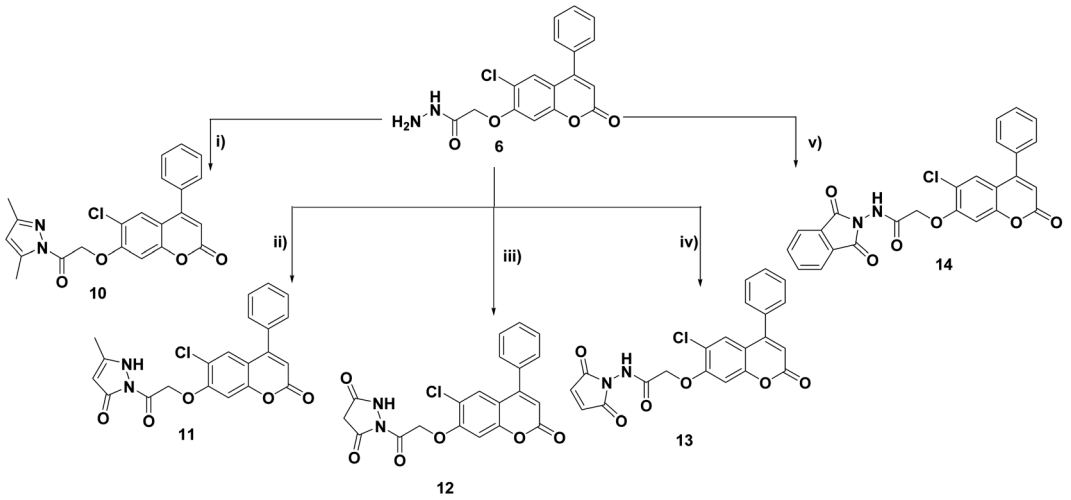

Scheme 3 Reagents and conditions: (i) $CH_3COCH_2COCH_3$, EtOH, reflux, 8 h; (ii) $CH_3COCH_2COOC_2H_5$, EtOH, reflux, 10 h; (iii) $CH_2(COOC_2H_5)_2$, AcOH, reflux, 12 h; (iv) maleic anhydride, AcOH, reflux, 6 h; (v) phthalic anhydride, AcOH, reflux, 8 h.

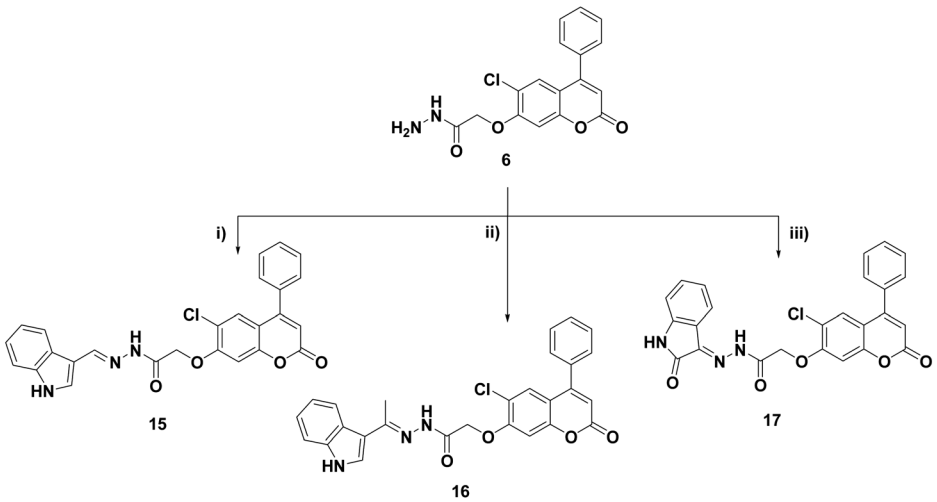

Scheme 4 Reagents and conditions: (i) 3-indole carbaldehyde, EtOH, AcOH, 6 h, reflux; (ii) 3-acetylindole, EtOH, AcOH, reflux, 6 h; (iii) isatin, EtOH, AcOH, reflux, 8 h.

compounds were confirmed by applying analytical and spectral methods, such as IR, MS, ^{1}H NMR and ^{13}C NMR.

2.2. Biological activity

2.2.1 Antimycobacterial screening

2.2.1.1 Antitubercular effects and cytotoxicity of the synthesized target compounds. All the target azaheterocyclic coumarin hybrids were assessed for their activity towards the tubercle bacilli, *M. tuberculosis* and nontuberculous mycobacteria *M. abscessus*. Primary screening showed that most of the tested compounds suppressed the growth of *M. tuberculosis* but not *M. abscessus* at 125 μg mL^{-1}. The minimal inhibitory concentration (MIC) was investigated for the active compounds against *M. tuberculosis* using MABA (microplate alamar blue assay) (Tables 1 and S1†). The tetrazole derivatives **4b** and **4c** showed the lowest MIC value of 15 μg mL^{-1}. The methylamino-1,3,4-oxadiazol compound **9a** inhibited the growth of *Mtb* H37Rv, displaying an MIC value of 31.25 μg mL^{-1}. The tetrazoles **3** and **4a**, thiadiazoles **8b,c** and their oxadiazole congeners **9b,c** in addition to the pyrazoles **11** and **12** and imide compounds **13** and **14** exhibited MIC values ranging from 62.5 to 125 μg mL^{-1}. Although the relationship between the structure of the target compounds and their anti-*Mtb* activity is not very clear, some points could still be concluded. The elongation of the dialkylamino side chain of the tetrazole derivatives could enhance the antitubercular effects; for example, diethylamino and morpholino derivatives **4b** and **4c** demonstrated more potent inhibition effects than the dimethylamino derivative **4a.** Similarly, ethylamino and phenylamino-thiadiazole compounds **8b** and **8c** showed moderate potency when compared to the methylamino derivative **8a**, which was devoid of any antitubercular effect. On the contrary, the presence of long alkylamino chains

Table 1 Antimycobacterial activity of tested compounds against *Mtb* H37Rv

Compounds	Mtb − MIC [μg mL^{-1}]	IC_{50}-L929 [μg mL^{-1}]	IC_{50}/MIC − Mtb
3	62.5	ND	ND
4a	62.5	ND	ND
4b	15	31.25	2
4c	15	125	8
8b	62.5	ND	ND
8c	62.5	ND	ND
9a	31.25	62.5	2
9b	62.5	ND	ND
9c	62.5	ND	ND
11	62.5	ND	ND
12	125	ND	ND
13	62.5	ND	ND
14	62.5	ND	ND
INH	0.05	—	—
ETH	0.25–16 (ref. 52)	—	—

or bulky groups on the oxadiazole derivatives showed reduced anti-TB effects; for example, the ethylamino-oxadiazole **9b** and phenylamino-oxadiazole **9c** derivatives were less potent than the methylamino-oxadiazole derivative **9a**. For the pyrazole-linked coumarin derivatives, methylpyrazol-5-one compound **11** was the most active, while the activity was dramatically reduced for 3,5-dioxopyrazole compound **12** and completely disappeared for 3,5-dimethylpyrazole derivative **10**. Moreover, compounds with acetohydrazide linker **15–17** lost any activity towards *Mtb*.

Compounds showing inhibition potential at concentrations ≤31.25 μg mL^{-1} were assessed for their cytotoxicity against mouse fibroblast cell line L929 using the MTT assay according to international standards (ISO 10993-5:2009(E)).[51] The determined IC_{50} value was about 8-fold higher for compound **4c** and 2 times higher for compounds **4b** and **9a** (Table 2). Considering the high selectivity index (SI) ratio of **4c** compared to derivatives **4b** and **9a** as well as to previously reported coumarin compounds,[34,35] compound **4c** was chosen for further biological assays.

*2.2.1.2 Antimycobacterial activity of **4c** against ΔkatG mutant.* Given that InhA enzyme is the target for the reference INH and the compounds tested in this study, the efficacy of the promising compound **4c** was assessed against ΔkatG mutant strain lacking the functional KatG enzyme, which shows resistance to INH. The promising anti-mycobacterial activity observed against the ΔkatG strain suggests that **4c** could be a potential candidate for future tuberculosis treatments (Table 2).

Table 2 Antimycobacterial activity of **4c** against Δ*katG* mutant

Compounds	Δ*katG* MIC [μg mL^{-1}]
4c	15
INH	200

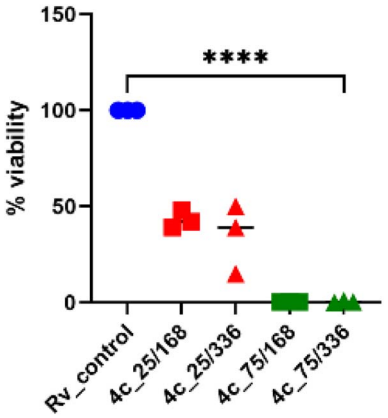

Fig. 4 Bactericidal effect of 4-phenylcoumarin **4c**. The tested compound was used at concentrations of 25 and 75 μg mL^{-1} for 7 (168 h) and 14 days (336 h), respectively. The number of viable bacteria was assessed through CFU analysis. Ordinary one-way ANOVA test was applied to compare control untreated *M. tuberculosis* (Rv_control) to bacilli treated with the tested compound at indicated concentrations and time points. The adjusted *p* value was <0.0001 for each pair comparison. The statistical analysis and graph were prepared using GraphPad Prism 9 version 9.3.1.

*2.2.1.3 Evaluation of the bactericidal activity of the target compound **4c**.* The bactericidal effect was evaluated for the promising compound **4c** by assessing the viability of bacteria exposed to the tested compound and by determining the number of colony-forming units (CFU). Compound **4c** displayed about 60% decrease in the viability of tubercle bacilli after 7 and 14 days of incubation at 25 μg mL^{-1} concentration and about 90% decrease at 75 μg mL^{-1} (Fig. 4).

*2.2.1.4 Assessment of the antimycobacterial activity of **4c** inside human macrophages.* Potential antimycobacterial drugs should be able to penetrate human macrophages to suppress the multiplication of *M. tuberculosis* that is located inside these phagocytic cells without causing lysis. Thus, the promising compound **4c** was evaluated for its activity towards tubercle bacilli inside human macrophages and cytotoxicity to human monocyte-derived macrophages (MDMs) in concentrations 2× and 4× MIC (Table S1†). Compound **4c** showed a significant decrease in the number of viable bacilli ($p = 0.0041$) compared to the untreated control (Fig. 5 and Table S2†), which proved its capability to cross the cell membrane.

*2.2.1.5 Assessment of the effectiveness of **4c** against mycobacterial biofilms. M. tuberculosis* can adhere to surfaces and develop biofilms that are important factors for antimicrobial resistance.[53] The potential new anti-tuberculosis agents should exhibit bactericidal effects against intra- or extracellular planktonic bacilli and against biofilm-forming bacteria. The bactericidal effect of compound **4c** on the *Mtb* biofilm formation was identified using a resazurin-based assay to determine the viability of the tubercle bacilli in tested and control untreated *Mtb* biofilm cultures. The presence of compound **4c** in the 2× MIC concentration decreased the biofilm viability by approximately 10% ($p < 0.0001$) (Fig. 6). Therefore, it seems that the tested compound **4c** has limited efficacy against biofilms

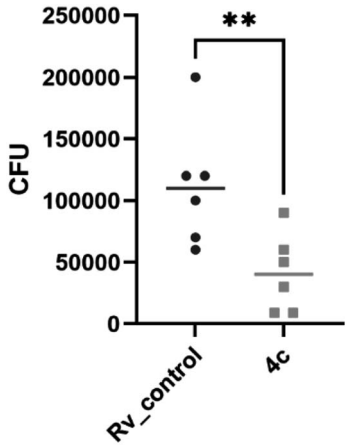

Fig. 5 Human monocyte-derived macrophages (MDMs) infected with *M. tuberculosis* and treated with compound **4c** in a 2× MIC concentration. Unpaired *t* test was applied to compare a number of intracellular *M. tuberculosis* (control) to bacilli treated with compound **4c**. The adjusted *p* value was determined as $p = 0.0041$. The statistical analysis was performed and the graph was prepared using GraphPad Prism 9 version 9.3.1.

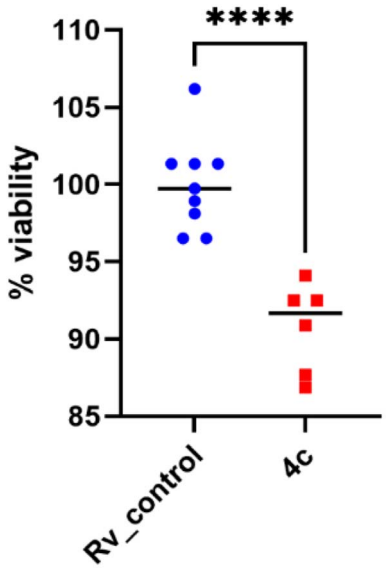

Fig. 6 Effect of compound **4c** on the mature biofilm composed of *M. tuberculosis*. Data were compared using unpaired *t* test. **** depicts the values with significant differences at $p < 0.0001$. The statistical analysis was performed and the graph was prepared using GraphPad Prism 9 version 9.3.1.

formed by *Mtb*, which may result from its greater bacteriostatic (MIC value) than bactericidal activity.

2.2.2 Inhibition of the *Mtb* InhA enzyme. Compound **4c** showing good activity against *M. tuberculosis* was further investigated for its potential inhibition of the InhA target enzyme. The results presented in Table 3 showed that compound **4c** was effectively able to inhibit InhA enzyme at a low micromolar concentration, displaying an IC_{50} of 0.56 μM superior to the reported reference drug triclosan ($IC_{50} = 0.73$ μM).

Table 3 InhA inhibition effect of the promising compound **4c**

Compound	IC_{50} (μM)
4c	0.565 ± 0.02
Triclosan	0.731 ± 0.03

2.3. Molecular docking

To predict the binding mode of the most active compound **4c** within the specified InhA active site, a molecular docking study was performed in which the co-crystallized ligand (PDB ID: 4TZK)[19] was used as a reference to compare the docking results of the examined compound **4c**. Docking was carried out in the presence of NAD cofactor, which participated in the recognition and binding of the co-crystalized ligand. The docking process was validated by redocking the co-crystallized ligand. The RMSD value of the redocked ligand was 0.5699 Å, which is a precise prediction of the favorable position. The co-crystallized ligand was able to create two hydrogen bonds with Tyr158 and Met161, as well as several hydrophobic interactions, and displayed a docking score of −9.5 kcal mol^{-1} (Fig. 7).

The most active compound, **4c**, occupied the active binding site in contact with the NAD, as demonstrated in Fig. 8, and displayed a strong binding affinity of −9.2 kcal mol^{-1}, which is about 0.3 kcal mol^{-1} less than that of the co-crystallized ligand (−9.5 kcal mol^{-1}). The coumarin core was observed to form π–π stacking interaction with Tyr158. The 4-phenylcoumarin system was found to interact hydrophobically with the non-polar pocket of the InhA active site, which includes Met103, Phe149, Gly104, Pro156, Met155, Tyr158, Ala157, Ile215, Ile202, Met199 and Leu218. Furthermore, the coumarin carbonyl oxygen atom was able to form an H-bonding interaction with the Gly104 residue. Compound **4c** and Tyr158 established one more H-bond *via* the tetrazole ring's nitrogen. As shown in Fig. 8, the tetrazole ring also established a π–sulfur interaction with Met161. Furthermore, **4c** maintained hydrophobic contact with NAD through its 2-morpholinoethyl tetrazole tail. In conclusion, **4c** displayed a strong binding affinity for the active site of InhA, matching the co-crystallized ligand that could clarify the modes of interaction of the recently synthesized candidates and contribute to the creation of new anti-tuberculosis agents.

2.4. Pharmacokinetics and physicochemical properties of compound 4c

The drug-likeness properties and parameters of the promising compound **4c** were predicted using the free web tool SwissADME, and some *in silico* descriptors and parameters were also calculated. The target compound **4c** displayed high gastrointestinal absorption with a moderate solubility profile and 0.55 bioavailability value, and it also showed no PAINS alerts. Furthermore, the investigated derivative was identified as a non-carcinogenic non-biodegradable compound (Table 4).

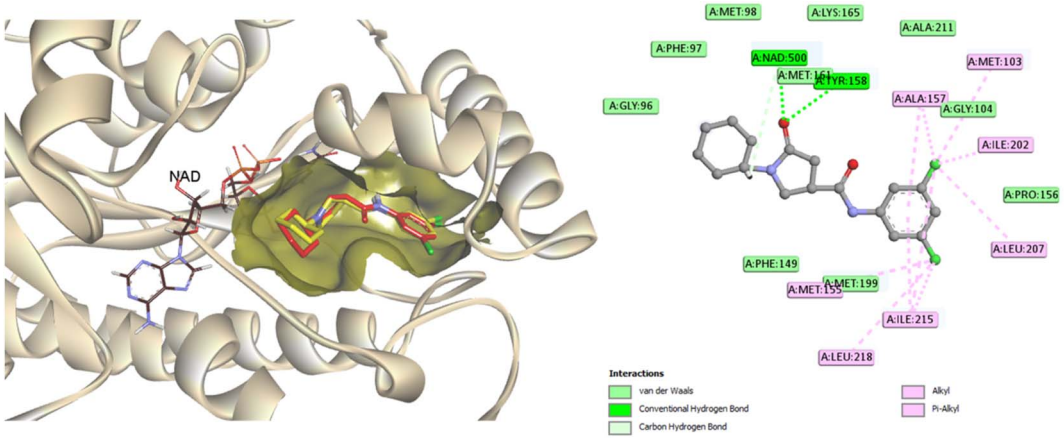

Fig. 7 2D interaction map and 3D overlay plot in the InhA protein active site (PDB ID: 4TZK) between co-crystallized (red) and redocked (yellow) ligands showing an RMSD of 0.5699 Å.

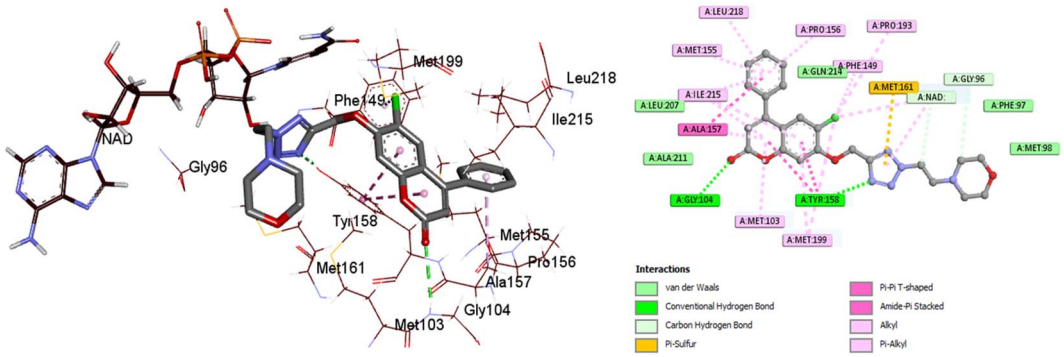

Fig. 8 2D and 3D interaction maps between InhA residues and ligand **4c**.

Table 4 Pharmacokinetics and physicochemical properties of compound **4c**

Compd	#Heavy atoms	#Rotatable bonds	#H-bond acceptors	#H-bond donors	MR	TPSA	WLOGP
4c	33	7	8	0	126.36	95.51	2.48

Compd	SOL class	GI absorption	Carcinogenicity	Lipinski #violations	Bioavailability score	PAINS #alerts	Biodegradation
4c	Moderately soluble	High	No	0	0.55	0	No

3. Conclusion

In this investigation, we designed and synthesized a series of coumarin derivatives bearing different azaheterocyclic rings to assess their effects against TB. The coumarin-tetrazole hybrid compound **4c** showed the highest potency against *Mtb* H37Rv, with an MIC value of 15 μg mL^{-1} and a favorable safety profile toward L929. It also inhibited the growth of the mutant strain (Δ*katG*) that is resistant to the reference drug INH. Moreover, compound **4c** was able to suppress the multiplication of *M. tuberculosis* inside human professional phagocytes and displayed low cytotoxicity against host cells. Compound **4c** was further evaluated for its inhibitory activity against InhA and exhibited significant activity at low micromolar concentration (IC_{50} = 0.565 μM). The binding mode of **4c** within InhA binding pocket was also investigated *via* molecular docking, which revealed that **4c** exhibited a strong binding affinity comparable to the reference compound ($\Delta G = -9.2$ kcal mol^{-1}), forming potential interactions with essential amino acids within the enzyme active site. Additionally, compound **4c** revealed favorable pharmacokinetic properties and obeyed Lipinski's rule. These findings confirm that compound **4c** could be considered

a promising antitubercular candidate endowed with characteristic inhibitory properties against the MTB InhA enzyme.

4. Materials and methods

4.1. Chemistry

All melting points were uncorrected and measured using the electrothermal IA 9000 apparatus. Infrared spectra (IR) were measured using a JASCO FT/IR-4100 spectrometer with KBr discs. The nuclear magnetic resonance spectra ^{1}H NMR (400 MHz) and ^{13}C NMR spectra (100 MHz) were recorded using a Bruker spectrometer with TMS as the internal standard. The mass spectrum was carried out on the Direct Inlet part of the mass analyzer in the Thermo Scientific GCMS model ISQ. The reactions were followed by TLC (silica gel, aluminum sheets 60 F254, Merck) using chloroform–methanol (9.5 : 0.5 v/v) as an eluent and sprayed with iodine-potassium iodide reagent. The purity of the newly synthesized compounds was assessed by TLC and elemental analysis and was found to be higher than 95%. The key intermediates **5**, **6** and **7a–c** were previously synthesized.[54]

4.1.1 General procedure for the preparation of 2-(6-chloro-2-oxo-4-phenyl-2*H*-chromen-7-yloxy)acetonitrile 2. To a solution of 6-chloro-7-hydroxy-4-phenylcoumarin **1** (2.72 g, 0.01 mol) in dry acetonitrile (30 mL), anhydrous potassium carbonate (1.38 g, 0.01 mol) was added, and the mixture was stirred at room temperature for 1 h. 2-Chloroacetonitrile (0.74 mL, 0.01 mol) was added, and the reaction mixture was heated at a reflux temperature for 8 h and then filtered. The filtrate was evaporated, and the remaining solid was collected and recrystallized from ethanol to produce compound **2**.

Yield 89%, mp 170–1 °C. Anal. calcd for $C_{17}H_{10}ClNO_3$ (311.72): C, 65.50; H, 3.23; N, 4.49. Found: C, 65.59; H, 3.31; N, 4.59. IR (cm^{-1}, KBr): 3053 (CH aromatic stretching), 2917 (CH aliphatic stretching), 2362 (C≡N), 1720 (C=O stretching). ^{1}H NMR (DMSO-d6, δ, ppm): 5.47 (2H, s, OCH_2), 6.43 (1H, s, H-3 coumarin), 7.42–7.61 (7H, m, Ar–H). ^{13}C NMR (DMSO-d6, δ, ppm): 55.36, 103.42, 114.03, 114.43, 116.21, 118.22, 127.75, 128.91, 129.53, 130.45, 134.37, 154.12, 154.28, 154.60, 159.78. MS *m*/*z* (R.A. %): 311, 313 (M^+, M^++2) (41.05, 12.61%), 115 (100.00%).

4.1.2 General procedure for the preparation of 7-((2*H*-tetrazol-5-yl)methoxy)-6-chloro-4-phenyl-2*H*-chromen-2-one 3. A mixture of compound **2** (3.1 g, 0.01 mol), sodium azide (0.65 g, 0.01 mol) and ammonium chloride (0.53 g, 0.01 mol) in *N*,*N*-dimethylformamide (30 mL) was heated for 7 h at 120 °C. The solvent was removed under reduced pressure, and the residue was dissolved in water (100 mL) and carefully acidified with conc. hydrochloric acid to pH ≈ 2. The solution was cooled to 0–5 °C in an ice bath in a refrigerator overnight, and the precipitated solid was filtered, washed with water, and recrystallized from an ethanol–water mixture (1 : 1) to give compound **3**.

Yield 85%, mp 259–60 °C. Anal. calcd for $C_{17}H_{11}ClN_4O_3$ (354.75): C, 57.56; H, 3.13; N, 15.79. Found: C, 57.66; H, 3.19; N, 15.86. IR (cm^{-1}, KBr): 3424 (NH stretching), 3105 (CH aromatic stretching), 2918 (CH aliphatic stretching), 1679 (C=O stretching). ^{1}H NMR (DMSO-d6, δ, ppm): 5.66 (2H, s, OCH_2), 6.25 (1H, s, H-3 coumarin), 7.01–7.58 (7H, m, Ar–H), 11.50 (1H, brs, NH, D_2O exchangeable). ^{13}C NMR (DMSO-d6, δ, ppm): 56.50, 104.36, 112.02, 117.47, 127.42, 128.80, 129.44, 130.27, 135.08, 154.19, 154.80, 157.09, 160.13. MS *m*/*z* (R.A. %): 354, 356 (M^+, M^++2) (2.83, 0.90%), 128 (100.00%).

4.1.3 General procedure for the preparation of 7-(5-[(2-(dimethylamino)ethylthio), 2-(diethylamino)ethylthio) and/or (2-morpholinoethylthio)]-1,3,4-oxadiazol-2-yl) methoxy)-4-phenyl-2*H*-chromen-2-one 4a–c. To a solution of tetrazole compound **3** (0.35 g, 0.001 mol), in dry acetonitrile (20 mL), anhydrous potassium carbonate (0.14 g, 0.001 mol) was added, and the mixture was stirred at room temperature for 1 hour. The appropriate aminoethyl chloride derivatives, namely 2-(dimethylamino)ethyl chloride hydrochloride, 2-(diethylamino)ethyl chloride hydrochloride, and/or 4-(2-chloroethyl) morpholine hydrochloride (0.001 mol), were added, and the reaction mixture was heated at reflux temperature for 8–10 hours and then filtered. The filtrate was evaporated, and the remaining solid was collected and recrystallized from ethanol to produce compound **4a–c**.

*4.1.3.1 7-((2-(2-(Dimethylamino)ethyl)-2H-tetrazol-5-yl) methoxy)-6-chloro-4-phenyl-2H-chromen-2-one **4a**.* Yield 76%; mp 87–8 °C. Anal. calcd for $C_{21}H_{20}ClN_5O_3$ (425.87): C, 59.23; H, 4.73; N, 16.44. Found: C, 59.31; H, 4.82; N, 16.52. IR (cm^{-1}, KBr): 3067 (CH aromatic stretching), 2919, 2851 (CH aliphatic stretching), 1725 (C=O stretching). ^{1}H NMR ($CDCl_3$, δ, ppm): 2.38 (6H, s, $2CH_3N$), 2.83–2.86 (2H, t, CH_2N), 4.19–4.22 (2H, t, CH_2S), 5.48 (2H, s, OCH_2), 6.25 (1H, s, H-3 coumarin), 6.93–7.54 (7H, m, Ar–H). ^{13}C NMR ($CDCl_3$, δ, ppm): 31.93, 47.82, 57.51, 68.11, 101.44, 112.75, 117.63, 127.50, 128.27, 129.01, 129.82, 134.73, 154.27, 154.65, 155.07, 155.82, 160.86. MS *m*/*z* (R.A. %): 425, 427 (M^+, M^++2) (27.7%, 9.1%), 167 (100.00%).

*4.1.3.2 7-((2-(2-(Diethylamino)ethyl)-2H-tetrazol-5-yl) methoxy)-6-chloro-4-phenyl-2H-chromen-2-one **4b**.* Yield 75%, mp 91–2 °C. Anal. calcd for $C_{23}H_{24}ClN_5O_3$ (453.92): C, 60.86; H, 5.33; N, 15.43. Found: C, 60.94; H, 5.39; N, 15.52. IR (cm^{-1}, KBr): 3061 (CH aromatic stretching), 2921, 2852 (CH aliphatic stretching), 1717 (C=O stretching). ^{1}H NMR ($CDCl_3$, δ, ppm): 1.28 (6H, m, $2\underline{CH_3}\ CH_2N$), 2.78 (4H, m, $2CH_3\underline{CH_2}N$), 3.31 (2H, t, CH_2N), 4.54 (2H, t, CH_2S), 5.51 (2H, s, OCH_2), 6.30 (1H, s, H-3 coumarin), 6.99–7.57 (7H, m, Ar–H). ^{13}C NMR ($CDCl_3$, δ, ppm): 14.12, 45.51, 46.03, 57.51, 68.11, 101.44, 112.86, 119.34, 127.50, 128.28, 129.06, 129.90, 134.95, 154.27, 154.94, 156.98, 160.62. MS *m*/*z* (R.A. %): 453, 455 (M^+, M^++2) (66.69%, 26.03%), 209 (100.00%).

*4.1.3.3 7-((2-(2-Morpholinoethyl)-2H-tetrazol-5-yl)methoxy)-6-chloro-4-phenyl-2H-chromen-2-one **4c**.* Yield 74%, mp 137–8 °C. Anal. calcd for $C_{23}H_{22}ClN_5O_4$ (467.9): C, 59.04; H, 4.74; N, 14.97. Found: C, 59.11; H, 4.83; N, 15.07. IR (cm^{-1}, KBr): 3057 (CH aromatic stretching), 2920, 2851 (CH aliphatic stretching), 1723 (C=O stretching). ^{1}H NMR (DMSO-d6, δ, ppm): 2.57 (4H, m, 2 CH_2N morpholine), 2.82 (2H, t, CH_2N), 4.33–4.36 (4H, t, 2 CH_2O morpholine), 3.58–3.60 (2H, t, CH_2S), 5.51 (2H, s, OCH_2), 6.34 (1H, s, H-3 coumarin), 7.35–7.60 (7H, m, Ar–H). ^{13}C NMR (DMSO-d6, δ, ppm): 54.00, 56.83, 60.06, 66.53, 68.31, 102.83, 112.75, 112.90, 118.28, 128.84, 129.50, 130.37, 134.89, 154.48,

154.58, 157.00, 160.06. MS *m*/*z* (R.A. %): 467, 469 (M^+, M^++2) (2.93%, 1.03%), 59 (100.00%).

4.1.4 Preparation of 7-((5-((methyl/ethyl and/or phenyl) amino)-6-chloro-1,3,4-thiadiazol-2-yl) methoxy)-4-phenyl-2*H*-chromen-2-one 8a–c. The appropriate thiosemicarbazides **7a**, **7b** and/or **7c** (0.001 mol) were dissolved in concentrated sulfuric acid (1.6 mL), cooled and allowed to stand for 30 minutes at 0 °C. The reaction mixture was gradually added to crushed ice. The separated solid was filtered off, washed with water till acid free and dried to afford the target compound **8a–c**.

*4.1.4.1 7-((5-(Methylamino)-1,3,4-thiadiazol-2-yl)methoxy)-6-chloro-4-phenyl-2H-chromen-2-one **8a**.* Yield 79%, mp 177–8 °C. Anal. calcd for $C_{19}H_{14}ClN_3O_3S$ (399.85): C, 57.07; H, 3.53; N, 10.51; S, 8.02. Found: C, 57.16; H, 3.61; N, 10.59; S, 8.12. IR (cm^{-1}, KBr): 3407 (NH stretching), 3107 (CH aromatic stretching), 2918, 2853 (CH aliphatic stretching), 1720 (C=O stretching). ^{1}H NMR (DMSO-d6, *δ*, ppm): 2.89 (3H, s, CH_3), 5.58 (2H, s, OCH_2), 6.36 (1H, s, H-3 coumarin), 7.36–7.84 (8H, m, Ar–H and NH). ^{13}C NMR (DMSO-d6, *δ*, ppm): 31.78, 66.20, 103.55, 113.34, 113.41, 118.39, 127.24, 128.83, 129.46, 130.36, 134.78, 152.35, 154.16, 154.39, 155.85, 159.89, 171.44. MS *m*/*z* (R.A. %): 399, 401 (M^+, M^++2) (100.00%, 29.86%).

*4.1.4.2 7-((5-(Ethylamino)-1,3,4-thiadiazol-2-yl)methoxy)-6-chloro-4-phenyl-2H-chromen-2-one **8b**.* Yield 86%, mp 142–3 °C. Anal. calcd for $C_{20}H_{16}ClN_3O_3S$ (413.88): C, 58.04; H, 3.90; N, 10.15; S, 7.75. Found: C, 58.12; H, 3.99; N, 10.22; S, 7.85. IR (cm^{-1}, KBr): 3442 (NH stretching), 3107 (CH aromatic stretching), 2918, 2850 (CH aliphatic stretching), 1722 (C=O stretching). ^{1}H NMR (DMSO-d6, *δ*, ppm): 1.16–1.19 (3H, t, CH_3), 3.29–3.31 (2H, m, CH_2), 5.58 (2H, s, OCH_2), 6.36 (1H, s, H-3 coumarin), 7.36–7.95 (8H, m, Ar–H and NH). ^{13}C NMR (DMSO-d6, *δ*, ppm): 14.62, 39.45, 66.16, 103.59, 113.38, 113.47, 118.39, 127.27, 128.85, 129.49, 130.38, 134.80, 152.24, 154.17, 154.43, 155.86, 159.91, 170.42. MS *m*/*z* (R.A. %): 413, 415 (M^+, M^++2) (6.58%, 2.16%), 114 (100.00%).

*4.1.4.3 7-((5-(Phenylamino)-1,3,4-thiadiazol-2-yl)methoxy)-6-chloro-4-phenyl-2H-chromen-2-one **8c**.* Yield 92%, mp 64–5 °C. Anal. calcd for $C_{24}H_{16}ClN_3O_3S$ (461.92): C, 62.40; H, 3.49; N, 9.10; S, 6.94. Found: C, 62.48; H, 3.57; N, 9.19; S, 7.02. IR (cm^{-1}, KBr): 3447 (NH stretching), 3056 (CH aromatic stretching), 2918 (CH aliphatic stretching), 1716 (C=O stretching). ^{1}HNMR (DMSO-d6, *δ*, ppm): 5.69 (2H, s, OCH_2), 6.37 (1H, s, H-3 coumarin), 6.99–7.63 (12H, m, Ar–H), 10.49 (1H, s, NH, D_2O exchangeable). ^{13}C NMR (DMSO-d6, *δ*, ppm): 66.06, 103.65, 113.42, 113.66, 116.96, 118.03, 118.40, 122.62, 127.10, 127.30, 128.84, 129.48, 129.56, 130.38, 134.78, 140.80, 141.00, 142.07, 154.18, 154.41, 154.55, 155.80, 159.91, 166.28. MS *m*/*z* (R.A. %): 461, 463 (M^+, M^++2) (19.86%, 7.23%), 57 (100.00%).

4.1.5 Preparation of 7-((5-(methyl/ethyl and/or phenyl-amino)-1,3,4-oxadiazol-2-yl)methoxy)-6-chloro-4-phenyl-2*H*-chromen-2-one derivative 9a–c. A solution of thiosemicarbazides **7a**, **7b** and/or **7c** (0.001 mol) in dry pyridine (20 mL) was refluxed for 10–14 h. The reaction mixture was left overnight at room temperature and gradually added to the crushed ice. The separated solid was filtered off, washed with water and dried to afford the target compounds **9a–c**.

*4.1.5.1 7-((5-(Methylamino)-1,3,4-oxadiazol-2-yl)methoxy)-6-chloro-4-phenyl-2H-chromen-2-one **9a**.* Yield 80%, mp 259–60 °C. Anal. calcd for $C_{19}H_{14}ClN_3O_4$ (383.79): C, 59.46; H, 3.68; N, 10.95. Found: C, 59.55; H, 3.73; N, 11.05. IR (cm^{-1}, KBr): 3445 (NH stretching), 3133 (CH aromatic stretching), 2917, 2850 (CH aliphatic stretching), 1677 (C=O stretching). ^{1}H NMR (DMSO-d6, *δ*, ppm): 2.86 (3H, s, CH_3), 5.58 (2H, s, OCH_2), 6.26 (1H, s, H-3 coumarin), 7.01–7.59 (7H, m, Ar–H), 11.55 (1H, s, NH, D_2O exchangeable). ^{13}CNMR (DMSO-d6, *δ*, ppm): 31.78, 66.24, 103.55, 113.36, 113.41, 118.39, 127.20, 128.85, 129.46, 130.34, 134.78, 152.35, 154.16, 154.38, 155.83, 159.89, 171.46. MS *m*/*z* (R.A. %): 383, 385 (M^+, M^++2) (53.32%, 16.68%), 306 (100.00%).

*4.1.5.2 7-((5-(Ethylamino)-1,3,4-oxadiazol-2-yl)methoxy)-6-chloro-4-phenyl-2H-chromen-2-one **9b**.* Yield 80%, mp 222–3 °C. Anal. calcd for $C_{20}H_{16}ClN_3O_4$ (397.81): C, 60.38; H, 4.05; N, 10.56. Found: C, 60.44; H, 4.11; N, 10.64. IR (cm^{-1}, KBr): 3442 (NH stretching), 3107 (CH aromatic stretching), 2918, 2850 (CH aliphatic stretching), 1679 (C=O stretching). ^{1}H NMR (DMSO-d6, *δ*, ppm): 1.26–1.29 (3H, t, CH_3), 3.29–3.31 (2H, m, CH_2), 5.54 (2H, s, OCH_2), 6.26 (1H, s, H-3 coumarin), 7.29–7.59 (7H, m, Ar–H), 11.55 (1H, s, NH, D_2O exchangeable). ^{13}C NMR (DMSO-d6, *δ*, ppm): 13.78, 37.84, 61.69, 103.59, 112.01, 113.51, 118.26, 127.45, 128.88, 129.46, 130.29, 134.80, 147.32, 154.20, 154.42, 155.52, 157.03, 159.90, 160.12. MS *m*/*z* (R.A. %): 397, 399 (M^+, M^++2) (39.59%, 13.15%), 145 (100.00%).

*4.1.5.3 7-((5-(Phenylamino)-1,3,4-oxadiazol-2-yl)methoxy)-6-chloro-4-phenyl-2H-chromen-2-one **9c**.* Yield 82%, mp 225–6 °C. Anal. calcd for $C_{24}H_{16}ClN_3O_4$ (445.85): C, 64.65; H, 3.62; N, 9.42. Found: C, 64.75; H, 3.70; N, 9.51. IR (cm^{-1}, KBr): 3424 (NH stretching), 3063 (CH aromatic stretching), 2918 (CH aliphatic stretching), 1716 (C=O stretching). ^{1}H NMR (DMSO-d6, *δ*, ppm): 5.56 (2H, s, OCH_2), 6.25 (1H, s, H-3 coumarin), 7.01–7.81 (12H, m, Ar–H), 11.55 (1H, s, NH, D_2O exchangeable). ^{13}C NMR (DMSO-d6, *δ*, ppm): 66.07, 103.65, 113.40, 113.56, 116.96, 118.03, 118.41, 122.62, 127.10, 127.28, 128.84, 129.49, 129.55, 130.38, 134.78, 140.80, 141.00, 142.06, 154.18, 154.42, 154.55, 155.80, 159.90, 166.30. MS *m*/*z* (R.A. %): 445, 447 (M^+, M^++2) (12.45%, 3.99%), 167 (100.00%).

4.1.6 Preparation of 7-(2-(3,5-dimethyl-1*H*-pyrazol-1-yl)-2-oxoethoxy)-6-chloro-4-phenyl-2*H*-chromen-2-one 10. A mixture of hydrazide **6** (0.34 g, 0.001 mol) and acetylacetone (0.001 mol, 0.1 mL) in 20 mL absolute ethanol was refluxed for about 8 hours while stirring. The formed precipitate after cooling was filtered, dried and crystallized from ethyl alcohol.

Yield 90%, mp 205–6 °C. Anal. calcd for $C_{22}H_{17}ClN_2O_4$ (408.83): C, 64.63; H, 4.19; N, 6.85. Found: C, 64.69; H, 4.27; N, 6.94. IR (cm^{-1}, KBr): 3118 (CH aromatic stretching), 2917, 2850 (CH aliphatic stretching), 1728, 1609 (C=O stretching). ^{1}HNMR (DMSO-d6, *δ*, ppm): 2.25 (3H, s, CH_3-pyrazole), 2.48 (3H, s, CH_3-pyrazole), 5.81 (2H, s, OCH_2), 6.28 (1H, s, CH-pyrazole), 6.34 (1H, s, H-3 coumarin), 7.38–7.61 (7H, m, Ar–H). ^{13}C NMR (DMSO-d6, *δ*, ppm): 14.01, 67.79, 103.26, 111.80, 113.21, 113.33, 118.24, 127.22, 128.87, 129.50, 130.37, 134.91, 144.25, 153.06, 154.23, 154.47, 156.53, 159.98, 167.35. MS *m*/*z* (R.A. %): 408, 410 (M^+, M^++2) (100.00%, 35.40%).

4.1.7 Preparation of 1-(2-(6-chloro-2-oxo-4-phenyl-2*H*-chromen-7-yloxy)acetyl)-1,2-dihydro-3-methylpyrazol-5-one 11. A mixture of hydrazide **6** (0.34 g, 0.001 mol) and ethylacetoacetate (0.001 mol, 0.13 mL) in 20 mL absolute ethanol was refluxed for about 10 hours while stirring. The formed precipitate after cooling was filtered, dried and crystallized from ethyl alcohol.

Yield 86%, mp 160–161 °C. Anal. calcd for $C_{21}H_{15}ClN_2O_5$ (410.81): C, 61.40; H, 3.68; N, 6.82. Found: C, 61.48; H, 3.77; N, 6.90. IR (cm^{-1}, KBr): 3434 (NH stretching), 3107 (CH aromatic stretching), 2918, 2851 (CH aliphatic stretching), 1731, 1695, 1610 (C=O stretching). ^1H NMR (DMSO-d6, δ, ppm): 3.37 (3H, s, CH_3-pyrazole), 5.28 (2H, s, OCH_2), 6.34 (1H, s, CH-pyrazole), 6.36 (1H, s, H-3 coumarin), 7.15–7.61 (7H, m, Ar–H), 10.78 (1H, s, NH, D_2O exchangeable). ^{13}C NMR (DMSO-d6, δ, ppm): 16.79, 66.74, 102.83, 112.98, 113.20, 118.24, 127.26, 128.86, 129.51, 130.38, 134.93, 148.76, 154.15, 154.55, 156.46, 159.99, 168.61, 169.92. MS *m*/*z* (R.A. %): 410, 412 (M^+, M^++2) (40.19%, 12.89%), 139 (100.00%).

4.1.8 Preparation of 1-(2-(6-chloro-2-oxo-4-phenyl-2*H*-chromen-7-yloxy)acetyl)pyrazolidine-3,5-dione 12. A mixture of hydrazide **6** (0.34 g, 0.001 mol) and diethylmalonate (0.001 mol, 0.15 mL) in glacial acetic acid (6 mL) was refluxed for 12 h. The reaction mixture was poured onto water, and the separated solid was collected, washed with water, and dried to obtain the target compound **12**.

Yield 82%, mp > 300 °C. Anal. calcd for $C_{20}H_{13}ClN_2O_6$ (412.78): C, 58.19; H, 3.17; N, 6.79. Found: C, 58.27; H, 3.26; N, 6.87. IR (cm^{-1}, KBr): 3250 (NH stretching), 3063 (CH aromatic stretching), 2919, 2851 (CH aliphatic stretching), 1714, 1638, 1603 (C=O stretching). ^1H NMR (DMSO-d6, δ, ppm): 3.71 (2H, s, CH_2 pyrazole), 4.34 (2H, s, OCH_2), 6.62 (1H, s, H-3 coumarin), 6.63–7.53 (7H, m, Ar–H), 12.00 (1H, s, NH pyrazole, D_2O exchangeable). ^{13}C NMR (DMSO-d6, δ, ppm): 55.71, 61.61, 103.98, 107.34, 115.37, 116.59, 118.78, 127.39, 135.81, 136.15, 141.88, 142.87, 145.70, 147.76, 149.81, 158.80, 160.99, 161.13, 161.95. MS *m*/*z* (R.A. %): 412, 414 (M^+, M^++2) (13.56%, 4.18%), 345 (100.00%).

4.1.9 Preparation of 2-(6-chloro-2-oxo-4-phenyl-2*H*-chromen-7-yloxy)-*N*-[(2,5-dioxo-2*H*-pyrrol-1(5*H*)-yl) and/or -(1,3-dioxoisoindolin-2-yl)]acetamides 13 and 14. To a solution of the hydrazide **6** (0.34 g, 0.001 mol) in glacial acetic acid (6 mL), the appropriate acid anhydrides, namely maleic and/or phthalic anhydride (0.001 mol), were added, and the mixture was refluxed for 6–8 h. The reaction mixture was cooled, and water was added to precipitate the target compounds, which were filtered, washed with water, dried, and crystallized from acetic acid.

*4.1.9.1 2-(6-Chloro-2-oxo-4-phenyl-2H-chromen-7-yloxy)-N-(2,5-dioxo-2H-pyrrol-1(5H)-yl) acetamide **13**.* Yield 82%, mp 221–2 °C. Anal. calcd for $C_{21}H_{13}ClN_2O_6$ (424.79): C, 59.38; H, 3.08; N, 6.59. Found: C, 59.46; H, 3.15; N, 6.68. IR (cm^{-1}, KBr): 3423 (NH stretching), 3061 (CH aromatic stretching), 2918 (CH aliphatic stretching), 1714, 1605 (C=O stretching). ^1H NMR (DMSO-d6, δ, ppm): 4.84 (2H, s, OCH_2), 6.21 (1H, s, H-3 coumarin), 7.00–7.59 (10H, m, Ar–H, CH pyrrole and NH). ^{13}C NMR (DMSO-d6, δ, ppm): 67.29, 111.59, 112.73, 117.74, 118.27, 127.27, 128.77, 129.43, 130.24, 134.90, 135.14, 154.29, 154.88, 156.94, 157.80, 160.02, 160.23. MS *m*/*z* (R.A. %): 424, 426 (M^+, M^++2) (15.19%, 5.55%), 127 (100.00%).

*4.1.9.2 2-(6-Chloro-2-oxo-4-phenyl-2H-chromen-7-yloxy)-N-(1,3-dioxoisoindolin-2-yl) acetamide **14**.* Yield 88%, mp 277–8 °C. Anal. calcd for $C_{25}H_{15}ClN_2O_6$ (474.85): C, 63.23; H, 3.18; N, 5.90. Found: C, 63.29; H, 3.26; N, 5.96. IR (cm^{-1}, KBr): 3426 (NH stretching), 3063 (CH aromatic stretching), 2918 (CH aliphatic stretching), 1736, 1671, 1604 (C=O stretching). ^1H NMR (DMSO-d6, δ, ppm): 5.14 (2H, s, OCH_2), 6.39 (1H, s, H-3 coumarin), 7.26–8.01 (11H, m, Ar–H), 11.09 (1H, s, NH, D_2O exchangeable). ^{13}C NMR (DMSO-d6, δ, ppm): 66.98, 103.23, 113.41, 113.58, 118.43, 124.33, 127.32, 128.85, 129.52, 129.85, 130.41, 134.80, 135.86, 154.12, 154.49, 156.20, 159.98, 165.33, 166.94. MS *m*/*z* (R.A. %): 474, 476 (M^+, M^++2) (7.10%, 2.56%), 209 (100.00%).

4.1.10 Preparation of *N*′-((1*H*-indol-3-yl) methylene/ethylidene)-2-(6-chloro-2-oxo-4-phenyl-2*H*-chromen-7-yloxy) acetohydrazide indole and 2-(6-chloro-2-oxo-4-phenyl-2*H*-chromen-7-yloxy)-*N*′-(3-oxoindolin-2-ylidene) acetohydrazide 15–17. To a mixture of the hydrazide compound **6** (0.34 g, 0.001 mol) in absolute ethanol (20 mL) containing glacial acetic acid (5 mL), different indole compounds (0.001 mol), indole-3-carbaldehyde, 3-acetylindole and/or isatin were added. The reaction mixture was refluxed for 6–8 hours. The formed precipitate was filtered while hot, washed with ethanol and dried to afford the title target compound **15–17**.

*4.1.10.1 N′-((1H-Indol-3-yl)methylene)-2-(6-chloro-2-oxo-4-phenyl-2H-chromen-7-yloxy) acetohydrazide **15**.* Yield 84%, mp > 300 °C. Anal. calcd for $C_{26}H_{18}ClN_3O_4$ (471.89): C, 66.18; H, 3.84; N, 8.90. Found: C, 66.26; H, 3.93; N, 8.99. IR (cm^{-1}, KBr): 3428, 3250 (NH stretching), 3061 (CH aromatic stretching), 2918 (CH aliphatic stretching), 2851 (CH = azomethine stretching), 1717, 1677 (C=O stretching), 1609 (C=N azomethine stretching). ^1H NMR (DMSO-d6, δ, ppm): 5.53 (2H, s, OCH_2), 6.34 (1H, s, H-3 coumarin), 7.12–8.17 (12H, m, Ar–H), 8.23 (1H, s, CH=N), 11.43 (1H, s, NH, D_2O exchangeable), 11.58 (1H, s, NH, D_2O exchangeable). ^{13}C NMR (DMSO-d6, δ, ppm): 66.86, 103.07, 111.75, 112.30, 112.95, 118.27, 121.04, 122.37, 123.10, 124.55, 127.12, 128.86, 129.51, 130.36, 131.12, 134.96, 137.55, 142.12, 145.54, 154.18, 154.58, 157.17, 160.02, 162.49, 167.39. MS *m*/*z* (R.A. %): 471, 473 (M^+, M^++2) (51.35%, 16.83%), 295 (100.00%).

*4.1.10.2 N′-(1-(1H-Indol-3-yl)ethylidene)-2-(6-chloro-2-oxo-4-phenyl-2H-chromen-7-yloxy) acetohydrazide **16**.* Yield 89%, mp 268–9 °C. Anal. calcd for $C_{27}H_{20}ClN_3O_4$ (485.92): C, 66.74; H, 4.15; N, 8.65. Found: C, 66.84; H, 4.22; N, 8.74. IR (cm^{-1}, KBr): 3372, 3114 (NH stretching), 3059 (CH aromatic stretching), 2917, 2850 (CH aliphatic stretching), 1715, 1680 (C=O stretching). ^1H NMR (DMSO-d6, δ, ppm): 2.33 (3H, s, CH_3), 5.55 (2H, s, OCH_2), 6.36 (1H, s, H-3 coumarin), 7.13–8.28 (12H, m, Ar–H), 10.71 (1H, s, NH, D_2O exchangeable), 11.49 (1H, s, NH, D_2O exchangeable). ^{13}C NMR (DMSO-d6, δ, ppm): 15.05, 67.41, 103.01, 112.11, 112.95, 115.16, 118.24, 120.85, 122.65, 123.74, 124.78, 127.15, 128.86, 129.06, 129.52, 130.38, 134.94, 137.63, 149.03, 154.17, 154.59, 157.10, 160.03, 168.15. MS *m*/*z* (R.A. %): 485, 487 (M^+, M^++2) (20.31%, 6.30%), 102 (100.00%).

4.1.10.3 2-(6-Chloro-2-oxo-4-phenyl-2H-chromen-7-yloxy)-N′-(3-oxoindolin-2-ylidene) acetohydrazide ***17****.* Yield 86%, mp > 300 °C. Anal. calcd for $C_{25}H_{16}ClN_3O_5$ (473.86): C, 63.37; H, 3.40; N, 8.87. Found: C, 63.44; H, 3.49; N, 8.96. IR (cm^{-1}, KBr): 3434, 3250 (NH stretching), 3061 (CH aromatic stretching), 2918 (CH aliphatic stretching), 1726, 1698, 1606 (C=O stretching). ^{1}H NMR (DMSO-d6, δ, ppm): 5.16, 5.62 (2H, 2s, OCH_2), 6.36 (1H, s, H-3 coumarin), 6.94–7.61 (11H, m, Ar–H), 11.27 (1H, s, NH, D_2O exchangeable), 13.53 (1H, s, NH, D_2O exchangeable). ^{13}C NMR (DMSO-d6, δ, ppm): 67.41, 103.27, 111.66, 113.05, 118.33, 120.12, 121.53, 123.12, 127.25, 128.87, 129.52, 130.40, 132.56, 134.84, 142.12, 154.19, 154.45, 159.96, 162.85, 167.39. MS *m*/*z* (R.A. %): 473, 475 (M^+, M^++2) (23.72%, 8.97%), 209 (100.00%).

4.2. Biology

4.2.1 Antitubercular activity

4.2.1.1 MIC determination. The minimal inhibitory concentration (MIC) for *M. tuberculosis* H37Rv and *M. abscessus* was determined in liquid 7H9/OADC (Middlebrook, Difco, Baltimore, MD, United States) media supplemented with various concentrations of the tested chemical agents. The compounds were dissolved in dimethyl sulfoxide (DMSO) and added directly to the growth medium. The final concentration of DMSO in the medium never exceeded 0.1% (vol/vol), and DMSO did not affect the growth of the bacilli. To define the MIC value, the Microplate Alamar Blue Assay (MABA test) was applied, as described by Franzblau *et al.*[55] The susceptibility of the tested strains was assessed based on the change in color from blue to pink based on visual inspection. Wells containing only bacteria, medium, or compound were used as controls in this experiment, and the MABA test was repeated independently three times.

4.2.1.2 In vitro cytotoxicity assay. Cytotoxicity assays were performed precisely according to international standards (ISO 10993-5:2009(E)) using L929 cells and the MTT assay. Additionally, for the selected compounds, cytotoxicity was determined against human monocyte-derived macrophages, but in this case, the cells were treated with the tested compounds for 48 h.

4.2.1.3 Bactericidal effect. The bacterial activity of the tested compounds was verified by measuring the optical density (OD600) of *M. tuberculosis* H37Rv cultures exposed to the selected compounds and by determining the number of colony-forming units (CFU). To obtain OD600 = 0.1, the *M. tuberculosis* H37Rv culture was diluted by adding liquid 7H9/OADC (Middlebrook, Difco, Baltimore, MD, United States) medium supplemented with 0.05% Tween 80. The appropriate amounts of compounds were added at the following concentrations: 25 μg mL^{-1} and 75 μg mL^{-1} for **4c** (2 repeats for each concentration). A bottle containing the culture without any compound represented the control for this experiment. The culture bottles were incubated at 37 °C. The optical density was measured after 7 and 14 days. The number of colony-forming units was determined by utilizing a solid 7H10/OADC (Middlebrook, Difco, Baltimore, MD, United States) medium with 0.5% glycerol. Mycobacteria from the bottles were diluted in liquid 7H9/OADC medium with 0.05% Tween 80 and cultured using prepared plates on day 1 and subsequently on days 7 and 14 of the experiment. After three to five weeks of incubation at 37 °C, the number of colonies (CFU) was counted.

4.2.1.4 Biofilm formation. The biofilm of *M. tuberculosis* was developed as described previously with minor modifications.[56] *M. tuberculosis* was cultured to an OD600 of 1 in 7H9/OADC supplemented with 0.05% tyloxapol. Next, the inoculum was added at a ratio of 1 : 100 v/v to Sauton's medium and dispensed into each well of a 24-well plate (2.5 mL per well), covered with a lid, protected with parafilm, and incubated in humidity at 37 °C for 5 weeks. Once the biofilm developed, the medium was replaced with fresh one supplemented with 0.1% casitone and the compounds in various concentrations, and it was further incubated at 37 °C for 48 h. The viability of the bacilli was determined by fluorescence measurements (excitation: 550 nm, emission: 590 nm) in the presence of resazurin (375 μl of 0.02% resazurin per well) after 90 min of incubation using the multimode microplate reader SpectraMax® i3 (Syngen). The results were expressed as the percent viability compared to the untreated *M. tuberculosis* biofilm.

4.2.1.5 Preparation of human MDMs, and evaluation of the bactericidal effect of the compounds on intracellularly growing tubercle bacilli. Human monocytes were isolated from commercially available (Regional Blood Donation Station, Lodz, Poland) and freshly prepared buffy coats from healthy human blood donors.[57,58] After washing the cultures of differentiated human monocyte-derived macrophages (MDMs) extensively to remove any nonadherent cells, they were rested overnight and incubated with a culture medium supplemented with various concentrations of the tested compounds. The viability of the macrophages was assessed after 48 h of incubation using 3-(4,5-dimethylthiazol-2-yl)-2,5-diphenyltetrazolium bromide (MTT) (Sigma, St. Louis, MO, United States). Additionally, the MDMs were infected with tubercle bacilli at an MOI of 1 : 10, as described by Korycka-Machala *et al.*[59] The bacteria outside the cells were removed by washing with a culture medium two hours after infection. Then, the samples were incubated for 1 h in a medium with 1 g per L gentamicin (Sigma, St. Louis, MO, United States) and rinsed three times with Iscove's medium with 2% human AB serum (Sigma, St. Louis, MO, United States). Next, a culture medium with or without (control) the test compounds at a concentration of 2× MIC was added to independent cultures of the infected macrophages, followed by incubation at 37 °C for 48 h under a humidified atmosphere of 10% CO_2-90% air. Finally, the macrophages were lysed with 0.1% SDS, and the number of CFUs (colony forming units) was determined as previously described.[60]

4.2.2 Evaluation of InhA inhibition. The inhibition of enoyl acyl carrier protein reductase (InhA) activity was evaluated following the previously reported method by Khalifa *et al.*[20]

4.3. Molecular modeling

From the RCSB PDB, the structural coordinates of the *M. tuberculosis* InhA protein were obtained in pdb format.[19] Except for NAD, non-protein moieties, including water, were removed, and hydrogen atoms were added using AutoDockTools.[61] The

2D and 3D geometric structures of **4c** were built using a Marvin Sketch. In the current docking study, AutoDock Vina was chosen to predict protein–ligand interactions and binding affinities.[62] The grid box size was 22.5 Å × 17.0 Å × 16.7 Å, with a position determined by the co-crystallized ligand's center (x, y, x; 9.6, 32.2, 60.7). Discovery Studio Visualizer was utilized for the analysis and visualization of the docking results.[63]

4.4. Pharmacokinetics and physicochemical properties

The free *SwissADME* web tool available from the Swiss Institute of Bioinformatics (SIB) and admetSAR 2.0 internet server were used to investigate some properties of the newly synthesized promising derivative **4c**. The structure of the compound was converted to a SMILES notation and then submitted to the online server for calculation.

Ethical approval

The study was conducted according to the appropriate ethical standards as required by guidance from The Medical Research Ethics Committee (MREC), Egypt, ethical clearance certificate no. 7445062022.

Data availability

The data supporting this article are included in ESI.†

Conflicts of interest

There are no conflicts of interest to declare.

Acknowledgements

JD was supported by the Ministry of Science and Higher Education, POL-OPENSCREEN, DIR/WK/2018/06 and National Science Centre, Poland UMO-2023/49/B/NZ7/01421.

References

1 J. Chakaya, M. Khan, F. Ntoumi, E. Aklillu, R. Fatima, P. Mwaba, N. Kapata, S. Mfinanga, S. E. Hasnain, P. D. M. C. Katoto, A. N. H. Bulabula, N. A. Sam-Agudu, J. B. Nachega, S. Tiberi, T. D. McHugh, I. Abubakar and A. Zumla, Global Tuberculosis Report 2020 - Reflections on the Global TB burden, treatment and prevention efforts, *Int. J. Infect. Dis.*, 2021, **113**, S7–S12.

2 J. Furin, H. Cox and M. Pai, Tuberculosis, *Lancet*, 2019, **393**, 1642–1656.

3 M. Pai, M. A. Behr, D. Dowdy, K. Dheda, M. Divangahi, C. C. Boehme, A. Ginsberg, S. Swaminathan, M. Spigelman, H. Getahun, D. Menzies and M. Raviglione, Tuberculosis, *Nat. Rev. Dis. Prim.*, 2016, **2**, 16076.

4 WHO, *Global tuberculosis report*, 2022, **https://www.who.int/teams/global-tuberculosis-programme/tb-reports/global-tuberculosis-report-2022**.

5 J. B. Lynch, Multidrug-resistant Tuberculosis, *Med. Clin. North Am.*, 2013, **97**, 553–579.

6 C. Lange, K. Dheda, D. Chesov, A. M. Mandalakas, Z. Udwadia and C. R. Horsburgh Jr, Management of drug-resistant tuberculosis, *Lancet*, 2019, **394**, 953–966.

7 C. A. Peloquin and G. R. Davies, The Treatment of Tuberculosis, *Clin. Pharmacol. Ther.*, 2021, **110**, 1455–1466.

8 Y. He, A. Fan, M. Han, Y. Zhang, Y. Tong, G. Zheng and S. Zhu, New perspectives on the treatment of mycobacterial infections using antibiotics, *Appl. Microbiol. Biotechnol.*, 2020, **104**, 4197–4209.

9 T. M. Walker, P. Miotto, C. U. Köser, P. W. Fowler, J. Knaggs, Z. Iqbal, M. Hunt, L. Chindelevitch, M. Farhat, D. M. Cirillo, I. Comas, J. Posey, S. V. Omar, T. E. Peto, A. Suresh, S. Uplekar, S. Laurent, R. E. Colman, C. M. Nathanson, M. Zignol, A. S. Walker, CRyPTIC Consortium, Seq&Treat Consortium, D. W. Crook, N. Ismail and T. C. Rodwell, The 2021 WHO catalogue of Mycobacterium tuberculosis complex mutations associated with drug resistance: A genotypic analysis, *Lancet Microbe*, 2022, **3**, e265–e273.

10 M. S. Prasad, R. P. Bhole, P. B. Khedekar and R. V. Chikhale, Mycobacterium enoyl acyl carrier protein reductase (InhA): A key target for antitubercular drug discovery, *Bioorg. Chem.*, 2021, **115**, 105242.

11 R. J. Kinsella, D. A. Fitzpatrick, C. J. Creevey and J. O. McInerney, Fatty acid biosynthesis in Mycobacterium tuberculosis: lateral gene transfer, adaptive evolution, and gene duplication, *Proc. Natl. Acad. Sci. U. S. A.*, 2003, **100**, 10320–10325.

12 W. Zhai, F. Wu, Y. Zhang, Y. Fu and Z. Liu, The Immune Escape Mechanisms of Mycobacterium Tuberculosis, *Int. J. Mol. Sci.*, 2019, **20**, 340.

13 A. Koul, E. Arnoult, N. Lounis, J. Guillemont and K. Andries, The challenge of new drug discovery for tuberculosis, *Nature*, 2011, **469**, 483–490.

14 S. L. Parikh, G. Xiao and P. J. Tonge, Inhibition of InhA, the enoyl reductase from Mycobacterium tuberculosis, by triclosan and isoniazid, *Biochemistry*, 2000, **39**, 7645–7650.

15 X. He, A. Alian and P. R. Ortiz de Montellano, Inhibition of the Mycobacterium tuberculosis enoyl acyl carrier protein reductase InhA by arylamides, *Bioorg. Med. Chem.*, 2007, **15**, 6649–6658.

16 P. Kamsri, N. Koohatammakun, A. Srisupan, P. Meewong, A. Punkvang, P. Saparpakorn, S. Hannongbua, P. Wolschann, S. Prueksaaroon, U. Leartsakulpanich and P. Pungpo, Rational design of InhA inhibitors in the class of diphenyl ether derivatives as potential anti-tubercular agents using molecular dynamics simulations, *SAR QSAR Environ. Res.*, 2014, **25**, 473–488.

17 M. E. Boyne, T. J. Sullivan, C. W. amEnde, H. Lu, V. Gruppo, D. Heaslip, A. G. Amin, D. Chatterjee, A. Lenaerts, P. J. Tonge and R. A. Slayden, Targeting fatty acid biosynthesis for the development of novel chemotherapeutics against Mycobacterium tuberculosis: evaluation of A-ring-modified diphenyl ethers as high-affinity InhA inhibitors, *Antimicrob. Agents Chemother.*, 2007, **51**, 3562–3567.

18 U. H. Manjunatha, S. P. S Rao, R. R. Kondreddi, C. G. Noble, L. R. Camacho, B. H. Tan, S. H. Ng, P. S. Ng, N. L. Ma, S. B. Lakshminarayana, M. Herve, S. W. Barnes, W. Yu,

K. Kuhen, F. Blasco, D. Beer, J. R. Walker, P. J. Tonge, R. Glynne, P. W. Smith and T. T. Diagana, Direct inhibitors of InhA are active against Mycobacterium tuberculosis, *Sci. Transl. Med.*, 2015, **7**, 269ra3.

19 X. He, A. Alian, R. Stroud and P. R. Ortiz de Montellano, Pyrrolidine carboxamides as a novel class of inhibitors of enoyl acyl carrier protein reductase from Mycobacterium tuberculosis, *J. Med. Chem.*, 2006, **49**, 6308–6323.

20 A. Khalifa, A. Khalil, M. M. Abdel-Aziz, A. Albohy and S. Mohamady, Isatin-pyrimidine hybrid derivatives as enoyl acyl carrier protein reductase (InhA) inhibitors against Mycobacterium tuberculosis, *Bioorg. Chem.*, 2023, **138**, 106591.

21 P. S. Shirude, P. Madhavapeddi, M. Naik, K. Murugan, V. Shinde, R. Nandishaiah, J. Bhat, A. Kumar, S. Hameed, G. Holdgate, G. Davies, H. McMiken, N. Hegde, A. Ambady, J. Venkatraman, M. Panda, B. Bandodkar, V. K. Sambandamurthy and J. A. Read, Methyl-thiazoles: a novel mode of inhibition with the potential to develop novel inhibitors targeting InhA in Mycobacterium tuberculosis, *J. Med. Chem.*, 2013, **56**, 8533–8542.

22 A. Campaniço, R. Moreira and F. Lopes, Drug discovery in tuberculosis. New drug targets and antimycobacterial agents, *Eur. J. Med. Chem.*, 2018, **150**, 525–545.

23 A. Sabt, M. A. Khedr, W. M. Eldehna, A. I. Elshamy, M. F. Abdelhameed, R. M. Allam and R. Z. Batran, New pyrazolylindolin-2-one based coumarin derivatives as anti-melanoma agents: design, synthesis, dual BRAFV600E/VEGFR-2 inhibition, and computational studies, *RSC Adv.*, 2024, **14**, 5907–5925.

24 T. K. Mohamed, R. Z. Batran, S. A. Elseginy, M. M. Ali and A. E. Mahmoud, Synthesis, anticancer effect and molecular modeling of new thiazolylpyrazolyl coumarin derivatives targeting VEGFR-2 kinase and inducing cell cycle arrest and apoptosis, *Bioorg. Chem.*, 2019, **85**, 253–273.

25 S. J. Hamid and T. Salih, Design, Synthesis, and Anti-Inflammatory Activity of Some Coumarin Schiff Base Derivatives: In silico and in vitro Study, *Drug Des., Dev. Ther.*, 2022, **16**, 2275–2288.

26 D. H. Dawood, R. Z. Batran, T. A. Farghaly, M. A. Khedr and M. M. Abdulla, New Coumarin Derivatives as Potent Selective COX-2 Inhibitors: Synthesis, Anti-Inflammatory, QSAR, and Molecular Modeling Studies, *Arch. Pharm.*, 2015, **348**, 875–888.

27 W. B. Li, X. P. Qiao, Z. X. Wang, S. Wang and S. W. Chen, Synthesis and antioxidant activity of conjugates of hydroxytyrosol and coumarin, *Bioorg. Chem.*, 2020, **105**, 104427.

28 N. A. A. Latif, R. Z. Batran, S. F. Mohamed, M. A. Khedr, M. I. Kobeasy, S. A. F. Al-Shehri and H. M. Awad, Synthesis, Molecular Docking and Dynamics Simulation Studies of New 7-oxycoumarin Derivatives as Potential Antioxidant Agents, *Mini-Rev. Med. Chem.*, 2018, **18**, 1572–1587.

29 S. Dhawan, P. Awolade, P. Kisten, N. Cele, A. S. Pillay, S. Saha, M. Kaur, S. B. Jonnalagadda and P. Singh, Synthesis, Cytotoxicity and Antimicrobial Evaluation of New Coumarin-Tagged beta-Lactam Triazole Hybrid, *Chem. Biodiversity*, 2020, **17**, e1900462.

30 R. Z. Batran, M. A. Khedr, N. A. A. Latif, A. A. Abd El Aty and A. N. Shehata, Synthesis, homology modeling, molecular docking, dynamics, and antifungal screening of new 4-hydroxycoumarin derivatives as potential chitinase inhibitors, *J. Mol. Struct.*, 2019, **1180**, 260–271.

31 M. Chebaiki, E. Delfourne, R. Tamhaev, S. Danoun, F. Rodriguez, P. Hoffmann, E. Grosjean, F. Goncalves, J. Azéma-Despeyroux, A. Pál, J. Korduláková, N. Preuilh, S. Britton, P. Constant, H. Marrakchi, L. Maveyraud, L. Mourey and C. Lherbet, Discovery of new diaryl ether inhibitors against Mycobacterium tuberculosis targeting the minor portal of InhA, *Eur. J. Med. Chem.*, 2023, **259**, 115646.

32 D. S. Reddy, M. Kongot and A. Kumar, Coumarin hybrid derivatives as promising leads to treat tuberculosis: Recent developments and critical aspects of structural design to exhibit anti-tubercular activity, *Tuberculosis*, 2021, **127**, 102050.

33 S. Srivastava, D. Bimal, K. Bohra, B. Singh, P. Ponnan, R. Jain, M. Varma-Basil, J. Maity, M. Thirumal and A. K. Prasad, Synthesis and antimycobacterial activity of 1-(β-d-Ribofuranosyl)-4-coumarinyloxymethyl-/-coumarinyl-1,2,3-triazole, *Eur. J. Med. Chem.*, 2018, **150**, 268–281.

34 Z. Q. Xu, W. W. Barrow, W. J. Suling, L. Westbrook, E. Barrow, Y. M. Lin and M. T. Flavin, Anti-HIV natural product (+)-calanolide A is active against both drug-susceptible and drug-resistant strains of Mycobacterium tuberculosis, *Bioorg. Med. Chem.*, 2004, **12**, 1199–1207.

35 I. Ahmad, J. P. Thakur, D. Chanda, D. Saikia, F. Khan, S. Dixit, A. Kumar, R. Konwar, A. S. Negi and A. Gupta, Syntheses of lipophilic chalcones and their conformationally restricted analogues as antitubercular agents, *Bioorg. Med. Chem. Lett.*, 2013, **23**, 1322–1325.

36 R. Z. Batran, E. Y. Ahmed, H. M. Awad, K. A. Ali and N. A. Abdel Latif, EGFR and PI3K/m-TOR inhibitors: design, microwave assisted synthesis and anticancer activity of thiazole-coumarin hybrids, *RSC Adv.*, 2023, **13**, 29070–29085.

37 R. Z. Batran, E. Y. Ahmed, E. S. Nossier, H. M. Awad and N. A. A. Latif, Anticancer activity of new triazolopyrimidine linked coumarin and quinolone hybrids: synthesis, molecular modeling, TrkA, PI3K/AKT and EGFR inhibition, *J. Mol. Struct.*, 2024, **1305**, 137790.

38 O. M. Abdelhafez, K. M. Amin, H. I. Ali, T. J. Maher and R. Z. Batran, Dopamine release and molecular modeling study of some coumarin derivatives, *Neurochem. Int.*, 2011, **59**, 906–912.

39 O. Ebenezer, M. A. Jordaan, G. Carena, T. Bono, M. Shapi and J. A. Tuszynski, An Overview of the Biological Evaluation of Selected Nitrogen-Containing Heterocycle Medicinal Chemistry Compounds, *Int. J. Mol. Sci.*, 2022, **2**, 8117.

40 N. Kerru, L. Gummidi, S. Maddila, K. K. Gangu and S. B. Jonnalagadda, A Review on Recent Advances in Nitrogen-Containing Molecules and Their Biological Applications, *Molecules*, 2020, **25**, 1909.

41 M. Zala, J. J. Vora and V. M. Khedkar, Synthesis, Characterization, Antitubercular Activity, and Molecular Docking Studies of Pyrazolylpyrazoline-Clubbed Triazole and Tetrazole Hybrids, *ACS Omega*, 2023, **8**, 20262–20271.

42 A. Foroumadi, F. Soltani, H. Moallemzadeh-Haghighi and A. Shafiee, Synthesis, in vitro-antimycobacterial activity and cytotoxicity of some alkyl alpha-(5-aryl-1, 3, 4-thiadiazole-2-ylthio) acetates, *Arch. Pharm.*, 2005, **338**, 112–116.

43 Y. Teneva, R. Simeonova, V. Valcheva and V. T. Angelova, Recent Advances in Anti-Tuberculosis Drug Discovery Based on Hydrazide-Hydrazone and Thiadiazole Derivatives Targeting InhA, *Pharmaceuticals*, 2023, **16**(4), 484.

44 L. Ballell Pages, J. Castro Pichel, R. Fernandez Menendez, E. P. Fernandez Velando, S. Gonzalez Del Valle, A. Mendoza Losana, and M. J. Wolfendale, (Pyrazol-3-yl)-1,3,4-thiadiazole-2-amine and (Pyrazol-3-yl)-1,3,4-thiazole-2-amine Compounds, WO2010/118852A1, PCT publication, 2010.

45 Y. Sajja, S. Vanguru, H. R. Vulupala, L. Nagarapu, Y. Perumal, D. Sriram and J. B. Nanubolu, Design, synthesis, and in vitro antituberculosis activity of benzo [6,7] cyclohepta[1,2-b]pyridine-1,3,4-oxadiazole derivatives, *Chem. Biol. Drug Des.*, 2017, **90**, 496–500.

46 J. Castro Pichel, R. Fernandez Menendez, E. P. Fernandez Velando, S. Gonzalez Del Valle, and A. Mallo-Rubio, 3-Amino-Pyrazole Derivatives Useful against Tuberculosis, WO2012/049161A1, PCT publication, 2012.

47 Z. Xu, C. Gao, Q. C. Ren, X. F. Song, L. S. Feng and Z. S. Lv, Recent advances of pyrazole-containing derivatives as anti-tubercular agents, *Eur. J. Med. Chem.*, 2017, **139**, 429–440.

48 H. Zhao, Y. Gao, W. Li, L. Sheng, K. Cui, B. Wang, L. Fu, M. Gao, Z. Lin, X. Zou, M. Jackson, H. Huang, Y. Lu and D. Zhang, Design, Synthesis, and Biological Evaluation of Pyrrole-2-carboxamide Derivatives as Mycobacterial Membrane Protein Large 3 Inhibitors for Treating Drug-Resistant Tuberculosis, *J. Med. Chem.*, 2022, **65**, 10534–10553.

49 N. G. Bajad, S. K. Singh, S. K. Singh, T. D. Singh and M. Singh, Indole: A promising scaffold for the discovery and development of potential anti-tubercular agents, *Curr. Res. Pharmacol. Drug Discov.*, 2022, **3**, 100119.

50 E. F. Khaleel, A. Sabt, M. Korycka-Machala, R. M. Badi, N. T. Son, N. X. Ha, M. F. Hamissa, A. E. Elsawi, E. B. Elkaeed, B. Dziadek, W. M. Eldehna and J. Dziadek, Identification of new anti-mycobacterial agents based on quinoline-isatin hybrids targeting enoyl acyl carrier protein reductase (InhA), *Bioorg. Chem.*, 2024, **144**, 107138.

51 A. Bekier, M. Kawka, J. Lach, J. Dziadek, A. Paneth, J. Gatkowska, K. Dzitko and B. Dziadek, Imidazole-Thiosemicarbazide Derivatives as Potent Anti-Mycobacterium Tuberculosis Compounds with Antibiofilm Activity, *Cells*, 2021, **10**, 3476.

52 P. Mugabo and M. Mulubwa, Ethionamide population pharmacokinetics/pharmacodynamics and therapeutic implications in South African adult patients with drug-resistant tuberculosis, *Br. J. Clin. Pharmacol.*, 2021, **87**, 3863–3870.

53 A. K. Ojha, A. D. Baughn, D. Sambandan, T. Hsu, X. Trivelli, Y. Guerardel, A. Alahari, L. Kremer, W. R. Jacobs Jr and G. F. Hatfull, Growth of Mycobacterium tuberculosis biofilms containing free mycolic acids and harbouring drug-tolerant bacteria, *Mol. Microbiol.*, 2008, **69**, 164–174.

54 R. Z. Batran, A. Sabt, M. A. Khedr, A. K. Allayeh, C. Pannecouque and A. F. Kassem, 4-Phenylcoumarin derivatives as new HIV-1 NNRTIs: Design, synthesis, biological activities, and computational studies, *Bioorg. Chem.*, 2023, **141**, 106918.

55 S. G. Franzblau, R. S. Witzig, J. C. McLaughlin, P. Torres, G. Madico, A. Hernandez, M. T. Degnan, M. B. Cook, V. K. Quenzer, R. M. Ferguson and R. H. Gilman, Rapid, low-technology MIC determination with clinical Mycobacterium tuberculosis isolates by using the microplate Alamar Blue assay, *J. Clin. Microbiol.*, 1998, **36**, 362–366.

56 M. Korycka-Machała, M. Kawka, J. Lach, R. Płocińska, A. Bekier, B. Dziadek, A. Brzostek, P. Płociński, D. Strapagiel, M. Szczesio, K. Gobis and J. Dziadek, 2,4-Disubstituted pyridine derivatives are effective against intracellular and biofilm-forming tubercle bacilli, *Front. Pharmacol*, 2022, **13**, 1004632.

57 M. Korycka-Machała, A. Viljoen, J. Pawełczyk, P. Borówka, B. Dziadek, K. Gobis, A. Brzostek, M. Kawka, M. Blaise, D. Strapagiel, L. Kremer and J. Dziadek, 1H-Benzo[d] Imidazole Derivatives Affect MmpL3 in Mycobacterium tuberculosis, *Antimicrob. Agents Chemother.*, 2019, **63**, e00441.

58 M. Kawka, A. Brzostek, K. Dzitko, J. Kryczka, R. Bednarek, R. Płocińska, P. Płociński, D. Strapagiel, J. Gatkowska, J. Dziadek and B. Dziadek, Mycobacterium tuberculosis Binds Human Serum Amyloid A, and the Interaction Modulates the Colonization of Human Macrophages and the Transcriptional Response of the Pathogen, *Cells*, 2021, **10**, 1264.

59 M. Korycka-Machała, A. Brzostek, B. Dziadek, M. Kawka, T. Popławski, Z. J. Witczak and J. Dziadek, Evaluation of the Mycobactericidal Effect of Thio-functionalized Carbohydrate Derivatives, *Molecules*, 2017, **22**, 812.

60 M. Korycka-Machała, J. Pawełczyk, P. Borówka, B. Dziadek, A. Brzostek, M. Kawka, A. Bekier, S. Rykowski, A. B. Olejniczak, D. Strapagiel, Z. Witczak and J. Dziadek, PPE51 Is Involved in the Uptake of Disaccharides by Mycobacterium tuberculosis, *Cells*, 2020, **9**, 603.

61 G. M. Morris, R. Huey, W. Lindstrom, M. F. Sanner, R. K. Belew, D. S. Goodsell and A. J. Olson, AutoDock4 and AutoDockTools4: Automated docking with selective receptor flexibility, *J. Comput. Chem.*, 2009, **30**, 2785–2791.

62 O. Trott and A. J. Olson, AutoDock Vina: improving the speed and accuracy of docking with a new scoring function, efficient optimization, and multithreading, *J. Comput. Chem.*, 2010, **31**, 455–461.

63 BIOVIA, and Dassault Systèmes, *Discovery Studio Visualizer, V24.0.0*, Dassault Systèmes, San Diego, 2024.